

Flexible Potentiostat Readout Circuit Patch for Electrochemical and Biosensor Applications

Pablo Escobedo, Libu Manjakkal, Markellos Ntagios, Ravinder Dahiya*

Bendable Electronics and Sensing Technologies (BEST), University of Glasgow, Glasgow, Scotland, G12 8QQ

*Correspondence to - Ravinder.Dahiya@glasgow.ac.uk

Abstract—This paper presents a miniaturized potentiostat readout circuit patch developed for electrochemical or biosensors. The presented patch has been fabricated on a flexible polyimide substrate using off-the-shelf electronics. In contrast to the traditional bulky equipment for electrochemical analysis, the presented patch is conformable and portable. As a proof of concept, the system has been used for pH measurements in buffer solution (6–8 pH values) with a printed thick film potentiometric pH sensor having platinum counter electrode. The obtained results are in line with a commercially available potentiostat that has been used for benchmarking.

Keywords—Biosensor, Potentiostat, Electrochemical Sensor, Amperometry, Flexible electronics, Flexible Printed Circuit Board.

I. INTRODUCTION

Sensor-laden wearable or electronic skin (eSkin) type systems have attracted huge interest in recent years because of the high potential they hold for self-health monitoring by measuring key health parameters [1]–[3]. In this regard, a wide range of techniques, both invasive and non-invasive, have been developed to sense number of health parameters within the body. Likewise several types of wearable sensors (physical, electrochemical, and biosensors etc.) have been explored as an alternative to the lab-based measurement systems, which capture compelling physiological data but are bulky and non-portable [4]–[8]. Further, in traditional hospital-based devices the patients are tethered to a monitoring device via cables [9], [10]. Continued research on this topic is expected to lead to widespread use of flexible electrochemical biosensors, allowing patients to monitor themselves, thus reducing the number of clinician contact hours [11]. To this end, it is important to develop non-obtrusive wearable systems with sensors and front-end electronics, low power electronics and wireless radio-communication interfaces on flexible and conformable substrates [5], [12]. This will also advance the commercially available wearable systems such as wristbands, smart watches etc. for measurement of heart rate, blood pressure, electrocardiogram, respiration rate, etc.

A key aspect of the development of wearable biosensors is making them portable by miniaturising the electronic circuits which retrieve and process physiological data [13]–[15]. The forms of hardware and circuitry used with wearable sensors depend on several factors including the sensor nature, the data transmission method (e.g. RFID/NFC, Bluetooth, etc.) and the environment they need to operate in. Flexible version of these circuits will lend themselves to a wide range of applications including conformable RFID tags [16], [17], robotic systems with skin-like sensing capabilities [18] and medical devices [7],

[19]. The immediate solution available for obtaining the bendable/flexible versions of electronics is based on flexible printed circuit boards (FPCB) with off-the-shelf electronic components. This FPCB based solution is akin to having mechanically integrated but otherwise distinct and stiff sub-circuit islands of off-the-shelf electronic components, connected to one another by metal interconnects [20]. Other solutions that are likely to benefit the field in medium to long-term are based on various novel (organic and inorganic) materials and methodologies (e.g. printed electronics, ultra-thin chip technologies etc.) [21], [22].

By using the FPCB based approach, herein we presented the flexible miniaturised three-electrode potentiostat readout circuit patch for biosensors monitoring. The presented patch has been fabricated on a flexible polyimide substrate as depicted in Figure 1. As a proof of concept, the presented readout circuit patch can retrieve a useful signal from a pH sensor with its peak currents automatically calculated for a range of pH values. The obtained experimental results have been compared with a reference device in the form of a commercially available potentiostat.

This paper is organised as follows: Section II describes the design of pH sensor and read out circuit. The fabrication method for FPCB is also described in this section along with the experimental set up for testing. Section III presents the results revealing the utility of developed patch for pH sensing in place of the traditional bulky and expensive commercial instruments. Finally, the key outcomes are summarized in Section IV.

II. MATERIALS AND METHODS

A. Circuit design and PCB fabrication

Potentiostats can be found in a number of biosensors measuring various parameters and can process information from two, three and four electrode sensor configurations. Figure 2 shows the block diagram of the complete system, including the

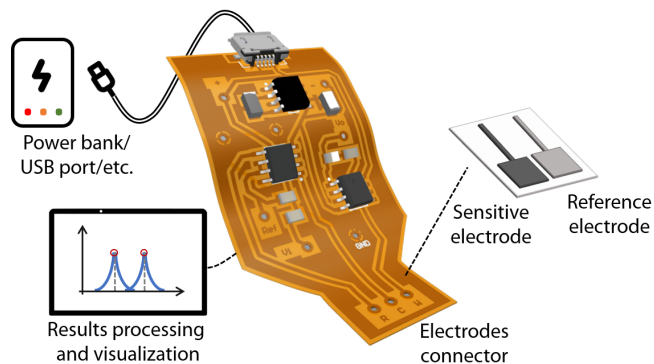


Fig. 1. Overview of the measurement system for electrochemical or biosensors.

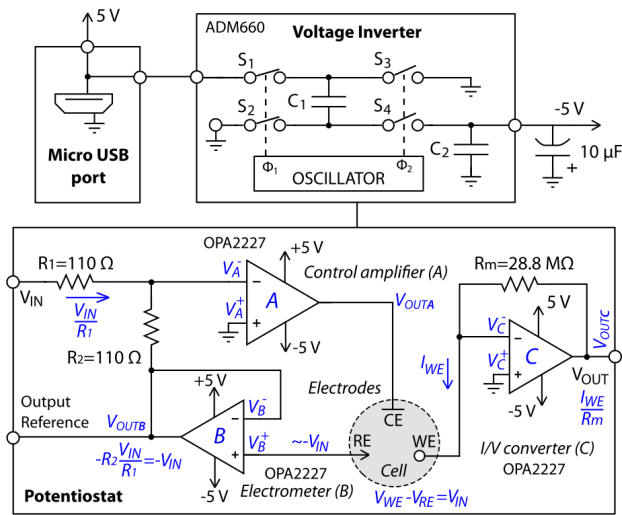


Fig. 2. Block diagram of the complete readout system including the micro USB port for powering, the voltage inverter and the potentiostat circuit.

schematic of the three-electrode potentiostat that is used in this work. Potentiostats measure the potential within a cell between the reference electrode (RE) and working electrode (WE). The current through the electrodes is minimised (ideally zero). The role of the counter electrode (CE) is to pass all the current needed to balance the current observed at the WE. Three-electrode potentiostats remedies some of the issues of the two-electrode configuration, such as measuring the potential changes of the WE independently of changes that may occur at the CE [23]. A potentiostat can be modelled as an electronic circuit consisting of four components: the control amplifier (A), the electrometer (B), the I/V converter (C), and the signal source. In summary, this circuit is designed to sense the potential difference between WE and RE. This is done at the voltage follower B (electrometer). The applied potential at WE is varied by changing V_{IN} at the control amplifier A. Since the output of B is the feedback signal to A, a change in V_{IN} away from the fixed potential of the RE causes A to force current into the electrochemical cell between CE and WE to balance the difference in the inputs at A. In this way, a pre-determined voltage is maintained between the WE and RE by sourcing current from the CE. The cell current flowing as a function of the changing potential output of the control amplifier is measured as a voltage drop across the feedback resistor R_m in the I/V converter. In our design, the electrometer, control amplifier and I/V converter are based on the OPA2227 precision bipolar operational amplifiers (Texas Instruments, Texas, USA). This device was selected due to its low offset voltage (75 μ V maximum) and drift. Since OPA2227 devices are dual supply op-amps, a supply voltage of ± 5 V is required for their operation. To that end, a voltage inverter based on the ADM660 integrated circuit (Analog Devices, USA) has been designed to obtain the negative voltage of -5 V from a positive 5 V supply. This chip has been chosen due to its low quiescent current (only 600 μ A) and the easy inverter configuration in which only two external capacitors are required. The positive supply of +5 V is directly obtained through a micro USB connector attached to the circuit, as shown in Figure 2. This can be connected for instance to a power bank supply or any generic USB supply port. The circuit layout was designed using Altium Designer 19.1.7 (Altium

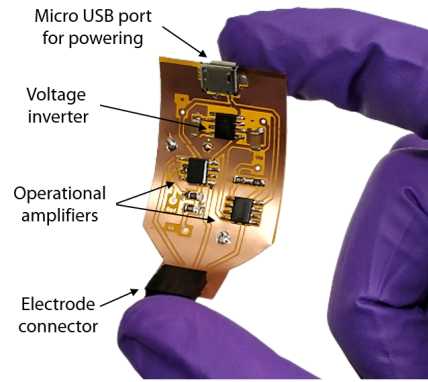


Fig. 3. Photograph of the circuit fabricated on flexible polyimide film substrate.

Limited, NSW, Australia). The PCB was fabricated using ultraviolet (UV) PCB etching on flexible polyimide film substrate coppered on one side and bonded together with a proprietary C-staged modified acrylic adhesive (AN210, C.I.F., Buc, France). The polyimide film has a thickness of 50 μ m. Metallization layer is copper 35 μ m thick. Figure 3 shows a photograph of the fabricated circuit.

B. Sensor description and fabrication

Several examples of the biosensors and their methods of detecting physiological parameters are given in Table I. As observed from Table I, most of the biosensors operate on the basis of potentiometry and amperometry techniques, which are types of electrochemical techniques. Electrochemical sensors react with the analyte of interest producing an electrical signal which is proportional to the analyte concentration [24]. A typical three-electrode based biosensor consists of a sensing electrode (SE) or WE, a CE and a RE separated by an electrolyte. Majority of applications implement a three-electrode system where the RE is connected to a high-input-impedance potentiostat circuit and a CE is used to complete the circuit for current flow [25]. Herein, we used pH sensors to validate the proof-of-concept readout circuit patch. We used thick film RuO_2 based sensitive and $\text{Ag}/\text{AgCl}/\text{KCl}$ reference electrodes on a ceramic substrate. The RuO_2 is used here because the metal oxides (MOx) based electrodes exhibit excellent sensitivity and selectivity for flexible and non flexible pH sensors [26]–[28]. The fabrication

TABLE I. EXAMPLES OF BIOSENSOR MEASUREMENT SYSTEMS

| Sensor | Biomarker | Transmission method | Sensing method | Ref |
|--------|---|---------------------|---|------------|
| Sweat | pH | Wired,RFID | Potentiometry | [5] [6] |
| Saliva | Uric acid | Bluetooth | Amperometry | [29] |
| Wound | Uric acid | RFID | Amperometry | [30] |
| Wound | Chitosan | Wired | Cyclic voltammetry | [31] |
| Blood | C-reactive protein | Wired | Magnetic | [32] |
| Blood | Glucose | RFID | Amperometry | [33] |
| N/A | Glucose, pH, H_2O_2 | RFID | Potentiometry, amperometry, cyclic voltammetry, ECL | [34] |
| Sweat | Glucose, Na^+ , K^+ , lactate | Bluetooth | Potentiometry, amperometry | [35] |
| Sweat | Glucose, pH, humidity | Wired | Impedimetric | [36] |

TABLE II. COMPARISON OF AVERAGE PEAK CURRENTS OBTAINED WITH PROPOSED READOUT CIRCUIT AND THE REFERENCE INSTRUMENT FOR 3 PH VALUES TESTED USING POTENTIOMETRY.

| pH value | Average peak current (μA) | |
|----------|--|----------------------|
| | Developed System | Reference Instrument |
| 6 | 28.9 | 29.9 |
| 7 | 32.8 | 29.7 |
| 8 | 26.6 | 26.6 |

of sensors is reported in a previous work [27]. To complete the circuit of the three electrode system, we used external Pt based commercial CE (Autolab). Further, for the miniaturized wireless sensing and online monitoring the electrodes were integrated with the developed potentiostat.

C. Experimental setup

A signal generator model WaveStation 3082 (Teledyne Lecroy, New York, USA) was used to generate the input signal for the potentiostat, which consists of a ramp voltage with a target peak voltage of 3.6 V. The output current was measured by placing a digital multimeter (DMM) model 34461A (Keysight Technologies, Santa Clara, CA, USA) on the output of the working electrode of the sensor, which was placed in the solution under test. A custom-made program in LabVIEW 2018 Robotics (National Instruments, Texas, USA) was used to visualize and monitor the measurements taken by the DMM. A commercial electrochemical workstation Autolab PGSTAT302N (Metrohm Autolab B.V., Utrecht, The Netherlands) was used in the study for benchmarking to evaluate the developed patch. The data collected was processed using Matlab (MathWorks, Massachusetts, USA) to automatically find the mean peak currents associated with each pH value.

III. RESULTS AND DISCUSSION

Figure 4 shows the experimental results obtained with the developed system and compared with the results from the reference instrument (i.e. commercial electrochemical workstation Autolab PGSTAT302N). The experiments were conducted for pH values from 6 to 8 using the pH sensor described in Section II. The detailed potentiometric performances (sensitivity 58 mV/pH and hysteresis of 10 mV (alkaline) and 3 mV (acidic)) of the sensor were presented in previous works[31]. The peak values of the currents are automatically identified and marked in the signals with red circles using the Matlab code previously described. Table II shows the average peak currents obtained for each pH value using both systems. It can be observed that the results are in good agreement in both systems. In the case of the pH 7 value, the peak current is slightly higher than expected in the developed system in comparison with the reference instrument. This high peak value could be due to the influence of the SE to neutral value of pH solution as compared pH 6 and pH 8 [27]. However, the same effect appears to occur, to a lesser extent, in the reference instrument, where the peak value for the pH 7 is similar to the obtained for the pH 6 value. Therefore, the anomalous increase observed with our system is indeed following to some extent the behaviour of the reference device.

IV. CONCLUSIONS

This work presents the design and fabrication of a miniaturized potentiostat readout circuit. As a proof of concept, the system was applied for pH sensing (pH values 6, 7 and 8).

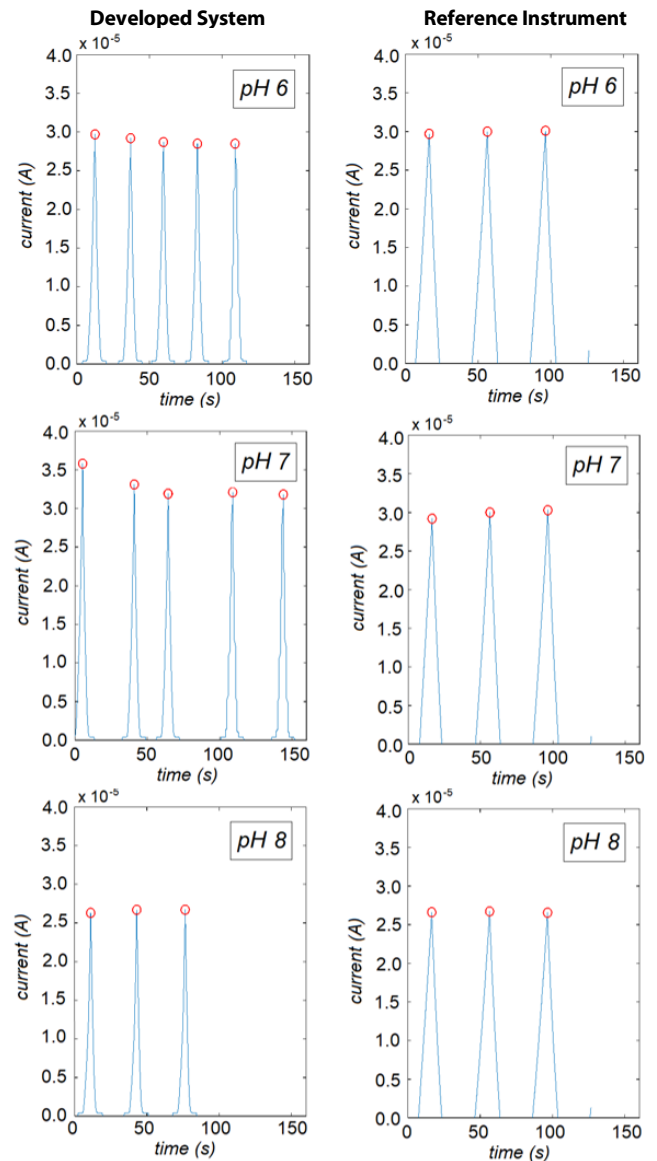


Fig. 4. Experimental results obtained with the developed system and the commercially available instrument used as reference for different pH values.

The obtained results are in agreement with a reference commercial potentiostat, so the developed system has potential to substitute the traditional bulky equipment for electrochemical analysis. The flexibility and portability of the system are in line with the current requirements of wearable biosensors to retrieve physiological data, making them more affordable and increasing the user satisfaction and acceptance. Future work will focus on the measurement of the sensor in wide pH range (2-12), as well as the sensing of other physiological parameters such as glucose or uric acid. In addition, a microcontroller-based circuit will be designed and included for conversion and communication.

ACKNOWLEDGEMENTS

This work was supported in North West Centre for Advanced Manufacturing (NW CAM) project supported by the European Union's INTERREG VA Programme (H2020-Interreg-IVA5055), managed by the Special EU Programmes Body (SEUPB). The views and opinions in this document do not necessarily reflect those of SEUPB.

REFERENCES

- [1] R. Dahiya, D. Akinwande, and J. S. Chang, "Flexible Electronic Skin: From Humanoids to Humans [Scanning the Issue]," *Proc. IEEE*, vol. 107, no. 10, pp. 2011–2015, Oct. 2019.
- [2] W. Gao, H. Ota, D. Kiriya, K. Takei, and A. Javey, "Flexible Electronics toward Wearable Sensing," *Acc. Chem. Res.*, vol. 52, no. 3, pp. 523–533, Mar. 2019.
- [3] S. B. Kim *et al.*, "Soft, skin-interfaced microfluidic systems with integrated enzymatic assays for measuring the concentration of ammonia and ethanol in sweat," *Lab Chip*, vol. 20, no. 1, pp. 84–92, 2020.
- [4] J. Kim, A. S. Campbell, B. E. De Ávila, and J. Wang, "Wearable biosensors for healthcare monitoring," *Nat. Biotechnol.*, vol. 37, no. April, 2019.
- [5] L. Manjakkal, W. Dang, N. Yogeswaran, and R. Dahiya, "Textile-Based Potentiometric Electrochemical pH Sensor for Wearable Applications," *Biosensors*, vol. 9, no. 1, p. 14, 2019.
- [6] W. Dang, L. Manjakkal, W. T. Navaraj, L. Lorenzelli, V. Vinciguerra, and R. Dahiya, "Stretchable wireless system for sweat pH monitoring," *Biosens. Bioelectron.*, vol. 107, no. December 2017, pp. 192–202, 2018.
- [7] E. S. Hosseini, L. Manjakkal, D. Shakthivel, and R. Dahiya, "Glycine-Chitosan Based Flexible Biodegradable Piezoelectric Pressure Sensor," *ACS Appl. Mater. Interfaces*, p. acsami.9b21052, Feb. 2020.
- [8] M. A. Kafi, A. Paul, A. Vilouras, and R. Dahiya, "Mesoporous chitosan based conformable and resorbable biostrip for dopamine detection," *Biosens. Bioelectron.*, vol. 147, no. October 2019, p. 111781, Jan. 2020.
- [9] P. Kassal, M. D. Steinberg, and I. M. Steinberg, "Wireless chemical sensors and biosensors: A review," *Sensors Actuators B Chem.*, vol. 266, pp. 228–245, Aug. 2018.
- [10] P. Escobedo *et al.*, "Smartphone-Based Diagnosis of Parasitic Infections With Colorimetric Assays in Centrifuge Tubes," *IEEE Access*, vol. 7, pp. 185677–185686, 2019.
- [11] A. Sun, A. G. Venkatesh, and D. A. Hall, "A Multi-Technique Reconfigurable Electrochemical Biosensor: Enabling Personal Health Monitoring in Mobile Devices," *IEEE Trans. Biomed. Circuits Syst.*, vol. 10, no. 5, pp. 945–954, Oct. 2016.
- [12] R. Fensli, P. E. Pedersen, T. Gundersen, and O. Hejlesen, "Sensor Acceptance Model – Measuring Patient Acceptance of Wearable Sensors," *Methods Inf. Med.*, vol. 47, no. 01, pp. 89–95, Jan. 2008.
- [13] J. P. de Campos da Costa, W. B. Bastos, P. I. da Costa, M. A. Zaghete, E. Longo, and J. P. Carmo, "Portable Laboratory Platform With Electrochemical Biosensors for Immunodiagnostic of Hepatitis C Virus," *IEEE Sens. J.*, vol. 19, no. 22, pp. 10701–10709, Nov. 2019.
- [14] Y. Montes-Cebrián *et al.*, "Competitive USB-Powered Hand-Held Potentiostat for POC Applications: An HRP Detection Case," *Sensors*, vol. 19, no. 24, p. 5388, Dec. 2019.
- [15] M. Simic, L. Manjakkal, K. Zaraska, G. M. Stojanovic, and R. Dahiya, "TiO₂-Based Thick Film pH Sensor," *IEEE Sens. J.*, vol. 17, no. 2, pp. 248–255, Jan. 2017.
- [16] R. Singh, E. Singh, and H. S. Nalwa, "Inkjet printed nanomaterial based flexible radio frequency identification (RFID) tag sensors for the internet of nano things," *RSC Adv.*, vol. 7, no. 77, pp. 48597–48630, 2017.
- [17] P. Escobedo *et al.*, "Flexible Passive Nfc Tag for Multi-Gas Sensing," *Anal. Chem.*, p. acs.analchem.6b03901, 2017.
- [18] M. Soni and R. Dahiya, "Soft eSkin: distributed touch sensing with harmonized energy and computing," *Philos. Trans. R. Soc. A Math. Phys. Eng. Sci.*, vol. 378, no. 2164, p. 20190156, Feb. 2020.
- [19] T. Bobrowski and W. Schuhmann, "Long-term implantable glucose biosensors," *Curr. Opin. Electrochem.*, vol. 10, pp. 112–119, 2018.
- [20] R. Dahiya, W. T. Navaraj, S. Khan, and E. O. Polat, "Developing Electronic Skin with the Sense of Touch," *Inf. Disp. (1975)*, vol. 31, no. 4, pp. 6–10, Jul. 2015.
- [21] C. García Núñez, F. Liu, W. T. Navaraj, A. Christou, D. Shakthivel, and R. Dahiya, "Heterogeneous integration of contact-printed semiconductor nanowires for high-performance devices on large areas," *Microsystems Nanoeng.*, vol. 4, no. 1, p. 22, Dec. 2018.
- [22] A. Zumeit, W. T. Navaraj, D. Shakthivel, and R. Dahiya, "Nanoribbons based Flexible High-Performance Transistors Fabricated at Room Temperature," *Adv. Electron. Mater.*, p. (in press), 2020.
- [23] D. Harvey, "Analytical Chemistry 2.0—an open-access digital textbook," *Anal. Bioanal. Chem.*, vol. 399, no. 1, pp. 149–152, Jan. 2011.
- [24] N. Bhalla, P. Jolly, N. Formisano, and P. Estrela, "Introduction to biosensors," *Essays Biochem.*, vol. 60, no. 1, pp. 1–8, Jun. 2016.
- [25] J. L. Hammond, N. Formisano, P. Estrela, S. Carrara, and J. Tkac, "Electrochemical biosensors and nanobiosensors," no. June, pp. 69–80, 2016.
- [26] L. Manjakkal, B. Sakthivel, N. Gopalakrishnan, and R. Dahiya, "Printed flexible electrochemical pH sensors based on CuO nanorods," *Sensors Actuators B Chem.*, vol. 263, pp. 50–58, Jun. 2018.
- [27] L. Manjakkal, B. Synkiewicz, K. Zaraska, K. Cvejic, J. Kulawik, and D. Szwagierczak, "Development and characterization of miniaturized LTCC pH sensors with RuO₂ based sensing electrodes," *Sensors Actuators B Chem.*, vol. 223, pp. 641–649, Feb. 2016.
- [28] L. Manjakkal, D. Szwagierczak, and R. Dahiya, "Metal oxides based electrochemical pH sensors: Current progress and future perspectives," *Prog. Mater. Sci.*, vol. 109, no. May 2019, p. 100635, 2019.
- [29] J. Kim *et al.*, "Wearable salivary uric acid mouthguard biosensor with integrated wireless electronics," *Biosens. Bioelectron.*, vol. 74, pp. 1061–1068, Dec. 2015.
- [30] P. Kassal *et al.*, "Smart bandage with wireless connectivity for uric acid biosensing as an indicator of wound status," *Electrochem. commun.*, vol. 56, pp. 6–10, Jul. 2015.
- [31] M. A. Kafi, A. Paul, A. Vilouras, E. S. Hosseini, and R. S. Dahiya, "Chitosan-Graphene Oxide based Ultra-thin and Flexible Sensor for Diabetic Wound Monitoring," *IEEE Sens. J.*, vol. PP, pp. 1–1, 2019.
- [32] M. H. F. Meyer *et al.*, "CRP determination based on a novel magnetic biosensor," vol. 22, pp. 973–979, 2007.
- [33] M. M. Ahmadi, G. A. Jullien, and L. Fellow, "A Wireless-Implantable Microsystem for Continuous Blood Glucose Monitoring," vol. 3, no. 3, pp. 169–180, 2009.
- [34] P. Escobedo *et al.*, "General-purpose passive wireless point-of-care platform based on smartphone," *Biosens. Bioelectron.*, vol. 141, no. March, p. 111360, 2019.
- [35] W. Gao *et al.*, "Fully integrated wearable sensor arrays for multiplexed in situ perspiration analysis," *Nature*, vol. 529, no. 7587, pp. 509–514, 2016.
- [36] H. Lee *et al.*, "Wearable/disposable sweat-based glucose monitoring device with multistage transdermal drug delivery module," *Sci. Adv.*, vol. 3, no. 3, p. e1601314, 2017.